UBY ILL – Lending
502532 Pages: 25 pages **ARIEL TXA**
Call (801) 422-8648 for resends.

ILLiad TN: 502532

Call #: Q 1 .A3 U64x

Location: 2ND

Journal Title: Technical report - Corps of Engineers, U.S. Army, Cold Regions Research and Engineering Laboratory.
ISSN:
Volume: Reseach Report 82 **Issue:**
Month/Year: 1961 **Pages:** 25 pages **ARIEL**

Article Author: Cold Regions Research and Engineering Laboratory (U.S.)
Article Title: Nakaya, U.; Elasric properties of processed snow with reference to its internal structure

ILL Number: 4013302

Lending String:
*UBY,CAI,NTE,LDL,IWA

Patron: santos, juan

Borrower: TXA
Texas A&M University
TAMU Libraries -Interlibrary Services
5000 TAMUS
College Station, TX 77843-5000
Fax: 979-862-4759
Ariel: 165.91.220.14
Odyssey:

BYU
BRIGHAM YOUNG UNIVERSITY

Harold B. Lee Library
Interlibrary Loan
Copy Center

For Ariel Receipt Problems:
Phone: 801-422-8648
Fax: 801-422-0464
Ariel: 128.187.229.251
Email: barbara_allred@byu.edu

Ariel Problem Report

If you have experienced a problem in the delivery of the requested item, please contact us within **Five Business Days** with the following information:

ILL#: _____
Your OCLC Symbol: _____
Date of Receipt: _____

Please specify if:

_____ Pages were Missing – pp._____ to _____
_____ Edges were Cut Off – pp._____ to _____
_____ Illegible Copy – Resend entire item
_____ Wrong Article Sent
_____ Other (Explain): _____

ELASTIC PROPERTIES OF PROCESSED SNOW WITH REFERENCE TO ITS INTERNAL STRUCTURE

by

Ukichiro Nakaya

Introduction

In the summer of 1957, the visco-elastic properties of snow in the Greenland Ice Cap were studied by the sonic method (Nakaya, 1959). In 1958, the visco-elastic properties of snow processed by the Peter snow miller were investigated with special reference to its age hardening (Nakaya, 1960). The experiments reported here were made in the summer of 1959 on snow processed by the Peter miller and the Snowblast miller at Site 2, 220 miles east of Thule, near 78°N latitude. The altitude is about 7000 ft.

In these experiments Young's modulus of various kinds of processed snow was measured as a function of density and age hardening. A thin section of each sample was made and the internal structure was examined. The samples were solidified in aniline at a temperature below -15C, and brought back in dry ice to the USA SIPRE laboratory in Wilmette, Illinois. Thin sections were made and photographed in the SIPRE laboratory. The mechanism of age hardening was clarified by examining the rate of increase of Young's modulus together with the mode of growth of bonds between ice grains, as revealed in thin section.

Experimental method

Young's modulus. Young's modulus was measured by the same visco-elastic meter as used in 1958. (For details see Nakaya, 1960). Young's modulus was measured as a function of density and time of age hardening. The loss factor was not measured.

Thin section method. The thin section of snow was made by a new method developed by Kinoshita and Wakahama (1959). This method is more convenient for observation of the internal structure of snow than Shimizu's method, which is described in a former report (Nakaya, 1960).

A sample of snow is immersed in liquid aniline at a temperature of about -8C and becomes soaked in a few seconds. When it is cooled down to about -15C, the air voids are filled with solid aniline, and the sample becomes a solid mass. In this state, the thin section can be easily made without destroying the bonds. The procedure is as follows: A flat surface is made by a microtome, and frozen to a glass plate by slightly melting the aniline and refreezing. A small quantity of water is added at the periphery of the sample to reinforce the bonding to the glass. Then the other side of the sample is cut to desired thickness on the microtome. The whole operation is done in a room at -20C. The thin section is put under a microscope in a room at -5C or so. The aniline soon melts and becomes transparent and photomicrographs (e.g., Fig. 1, 2) can be taken.

To get a general idea of grain distribution and mode of bonding, the proper thickness may be about half the mean grain size. Figure 1 shows a sample of hard, naturally compacted snow, from a depth D of 185 cm in the ice cap. The mean grain size is about 0.5 mm. This sample was cut to a thickness d = 0.22 mm, about half the mean grain size. The small spheres are air bubbles which must be disregarded. The advantage of this relatively thick section is not only that the mode of bonding is revealed clearly but also that the grain size is shown in three dimensions. When the section is too thin, the three-dimensional size distribution must be inferred. The formulation of this problem has been done by Jellinek (1957) and many others, but the calculation is time-consuming. The simplest way of obtaining the approximate three-dimensional size distribution is to examine a relatively thick section of snow. After photographing the thicker section (Fig. 1) the sample is refrozen and the thickness reduced to d = 0.80 mm (Fig. 2). Some grains are lost in this thinner section, but the nature of bonding is more clearly seen as shown by arrows. The bond diameter is of the order of 0.1 or 0.15 mm. The thinner section is better for examining the nature of the smaller bonds.

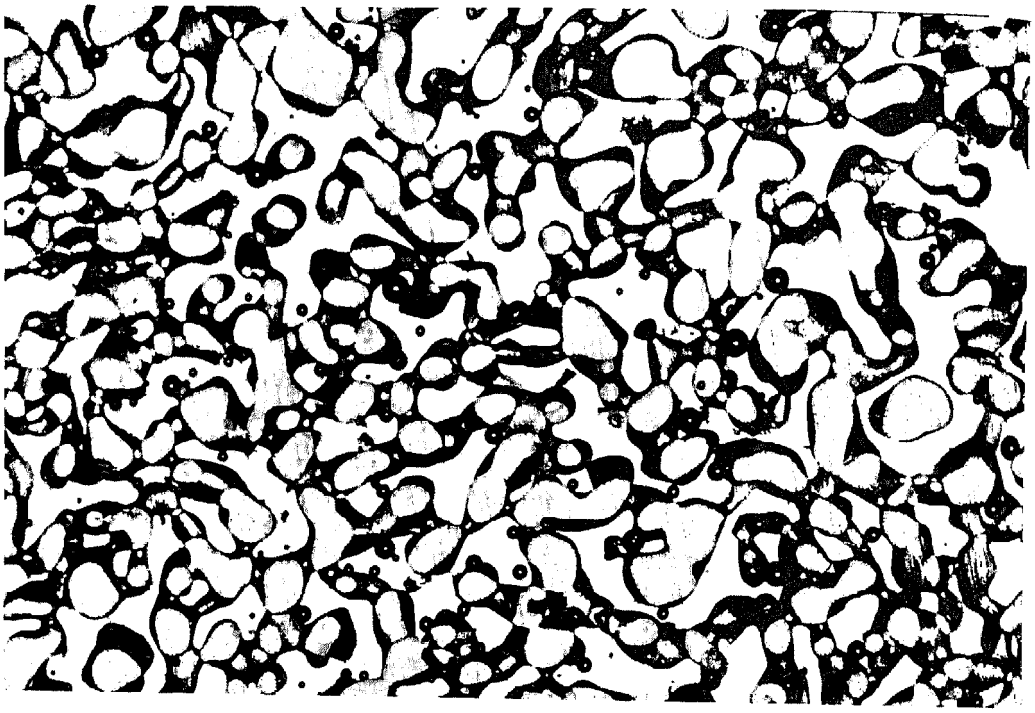

Figure 1. Naturally compacted snow; settled hard, D = 1.85 m. ρ = 0.448 g/cm^3, d = 0.22 mm, x 14.8, no. 509.

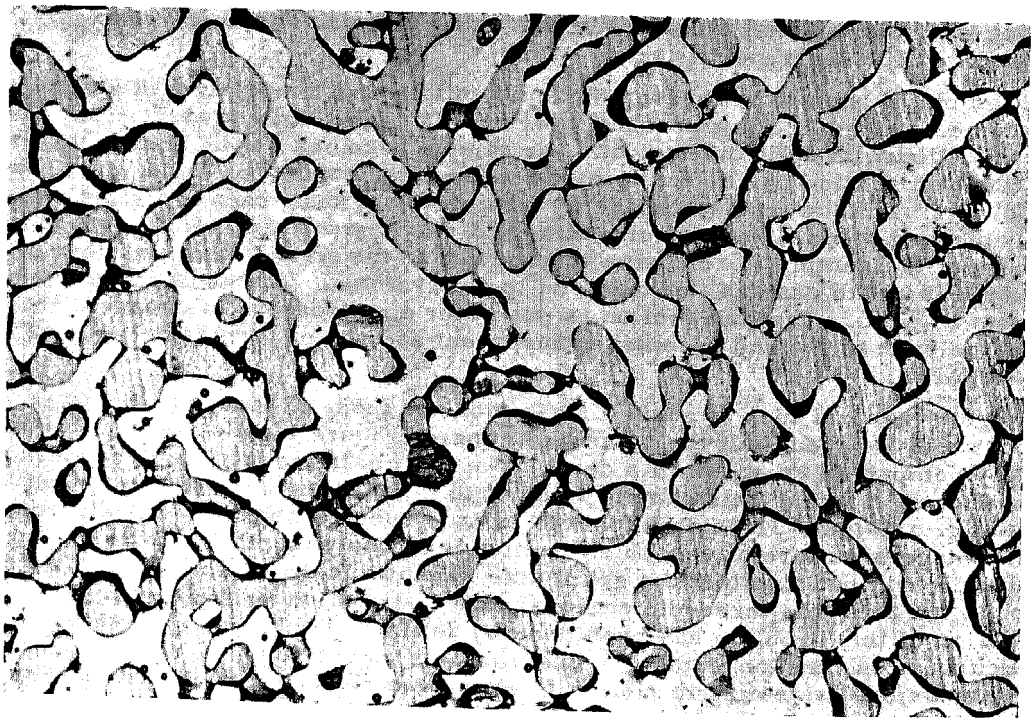

Figure 2. Same sample as Fig. 1 after refreezing and reducing thickness, d = 0.08 mm, x 14.8, no. 511.

Samples investigated. Snow blown and deposited by a snow miller (processed snow) becomes hardened with time, usually fairly rapidly. The Peter snow miller and the Snowblast miller were used for processing in the summer of 1959.

The Snowblast miller has a different disaggregating miller than the Peter apparatus and has a semi-circular chute erected vertically so that the snow takes a semi-circular path along the chute and hits the ground. The density of snow processed by the Snowblast miller (designated SB) is greater than snow processed by the Peter miller (PS). More fine particles are captured in SB than in PS and this seems more favorable for the hardening of processed snow, as described in an earlier report (Nakaya, 1960). Some of the processed snows were mechanically compacted, but others were left undisturbed.

Some samples of Peter snow deposits made in 1958 and left in the field for one year were examined. Other samples were left in the undersnow laboratory for one year. They were preserved in plastic bags and the shape of sample was kept almost unchanged. Young's modulus was measured for these samples and compared with that measured one year ago. The samples are listed in Table I.

Table I. Sample data.

Nature of processed snow	Undisturbed	Compacted
SB: new deposit	A, B, D	C, F
PS: new deposit	E, M, P, I, N	-------
PS: 1 year in the field	O	H, H', K, K'
PS: 1 year in the laboratory	V, W, X, Y, Z, a, b, e, f, g, h, ℓ	-------

Elastic properties and internal structure of snow processed by Snowblast miller

Snow profile. The profile of a snow deposit processed by the Snowblast miller is shown in Figure 3. When the deposit is undisturbed (series A, Fig. 3) both density ρ and Young's modulus E increase with depth. The parallel is fairly good, which shows that Young's modulus is proportional to density. When the deposit is mechanically compacted (series F, Fig. 3) both Young's modulus and density are high in the layer near the surface. The density increases to 0.61 in the layer 10 cm below the surface. This is the highest density hitherto obtained in processed snow. The highest density obtained in 1958 was 0.58 g/cm³ for vibrated Peter snow and 0.55 for compacted Peter snow. As a first approximation, Young's modulus is proportional to density. The Snowblast miller with the back chute, was therefore more effective for snow compaction than the Peter miller. The density of undisturbed and compacted snow becomes almost the same 50 cm below the surface. Compaction seems to be effective to a depth of about 50 cm.

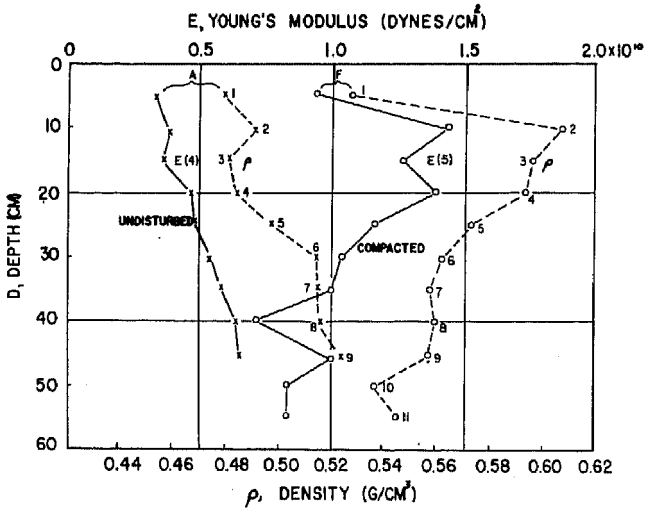

Figure 3. Profile of Young's modulus and density in snow processed by Snowblast miller.

Relation between Young's modulus and density. Snow processed by the Snowblast miller was similar to the Peter snow observed in summer 1958 in the relation between Young's modulus E and density ρ and in the mode of age hardening. The E-ρ relation for undisturbed Snowblast snow, A-series, is shown in Figure 4. The E-ρ relation for naturally compacted snow (dashed line, Fig. 4) is taken as the standard curve

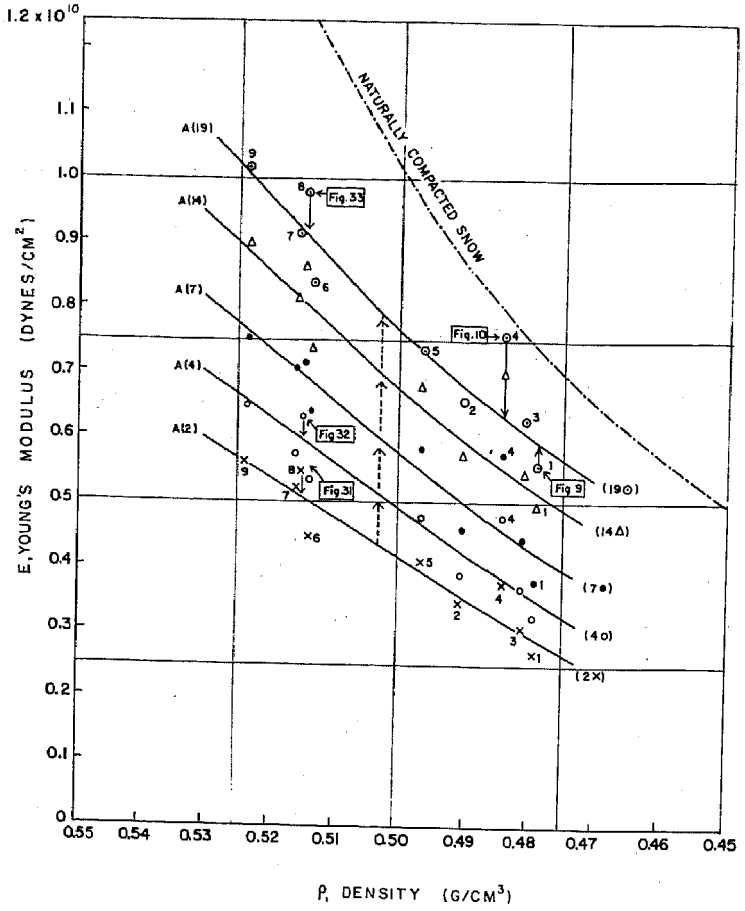

Figure 4. E-ρ relation for A-series SB undisturbed. (Nos. in parenthesis indicate days of age hardening).

fo. discussion of the E-ρ relation of any processed snow. The characteristic of this standard curve is that the E-ρ relation is expressed by a straight line for densities above 0.5 g/cm³ and shows an exponential form for densities below 0.5, as explained in full detail previously (Nakaya, 1959).

For processed snow also, $\underline{E}$ is proportional to ρ in the density range above 0.5. This point was not very noticeable in the previous experiments, because the data in the region of higher densities were not sufficient. When the Snowblast snow is mechanically compacted, the density increases to 0.61, and the straight part of the E-ρ curve is clearly demonstrated. One example is shown in Figure 5. The empirical formula of the straight line is

$$E = k\,(\rho - 0.5) + E_{0.5}$$

in which $\underline{E}_{0.5}$ is Young's modulus at $\rho = 0.5$. Figures 4 and 5 show that $\underline{E}_{0.5}$ increases gradually with time for both compacted and undisturbed snow. The value of $\underline{k}$ also increases with time for the undisturbed snow, but is almost constant for compacted snow. The time dependence of $\underline{E}_{0.5}$ and $\underline{k}$, from Figures 4 and 5, is shown in Figure Each curve increases with time with the standard curve of naturally compacted snow as its asymptote.

Young's modulus and internal structure. The observed data show some scattering along the E-ρ curve (Fig. 4, 5), but it was noted that values for a given sample are consistently higher or lower than the average for each stage of age hardening. For

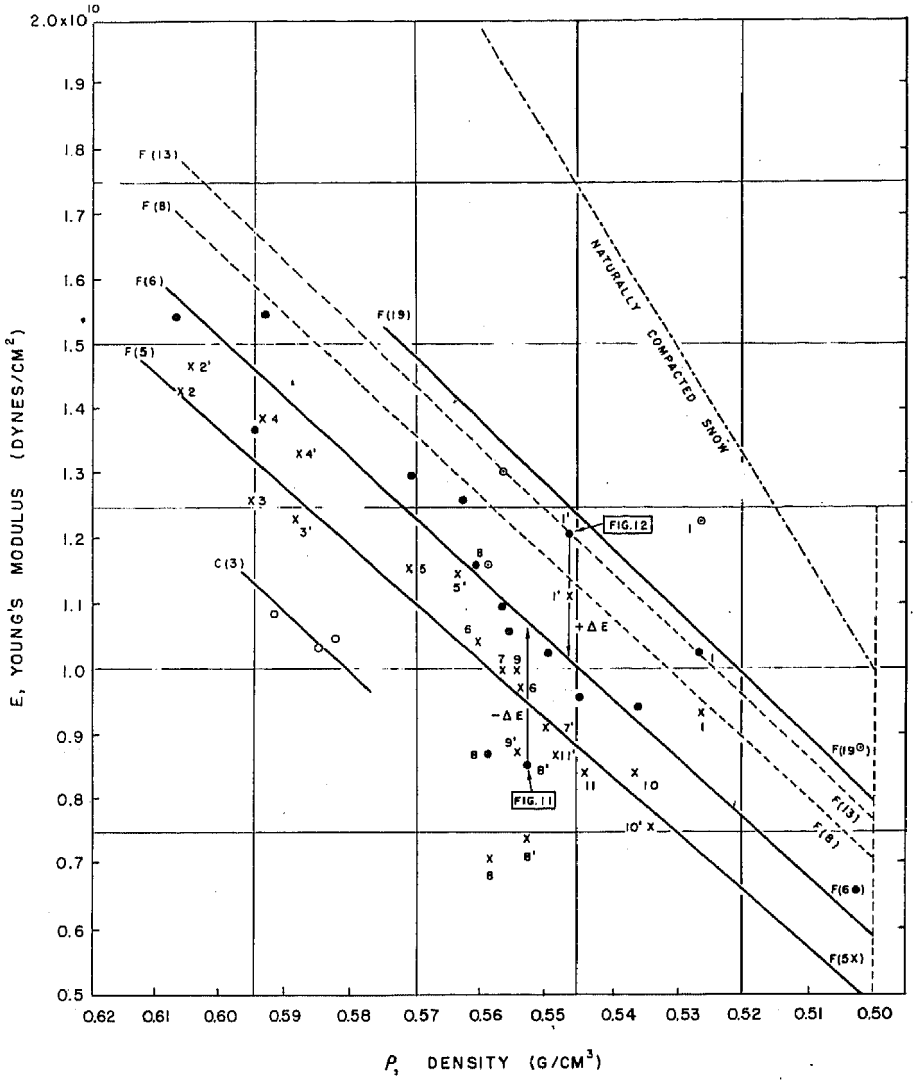

Figure 5. E-ρ relation for F-series SB compacted.

example, no. 4 in Figure 4 and no. 1 in Figure 5 show markedly higher values than the average at each stage of age hardening, and no. 1 in Figure 4 and no. 8 in Figure 5 are always lower. The deviation ΔE from the E-ρ curve is expressed by α,

$$\alpha = \frac{E+\Delta E}{E} \quad \text{or} \quad \Delta E = (\alpha - 1)\, E.$$

For a given density:

$\alpha > 1$, $\Delta E > 0$; stronger bonding between grains than the normal state,

$\alpha = 1$, $\Delta E = 0$; observed data lie on E-ρ curve,

$\alpha < 1$, $\Delta E < 0$; weaker bonding between grains than the normal state.

Thus α can be taken as a measure of the internal structure of snow. In Figure 7, α for A(2) and A(19) of undisturbed Snowblast snow is plotted as the function of depth in the deposit. The two curves coincide almost perfectly. Therefore, the deviation from the E-ρ curve is inherent in the sample, indicating that this deviation is due to the difference in the internal structure. No simple relation is observed between this structure

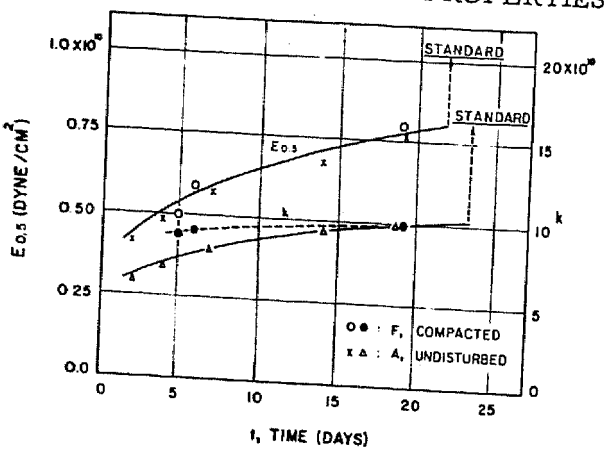

Figure 6. Time dependence of $\underline{E}_{0.5}$ and $\underline{k}$, compacted and undisturbed SB.

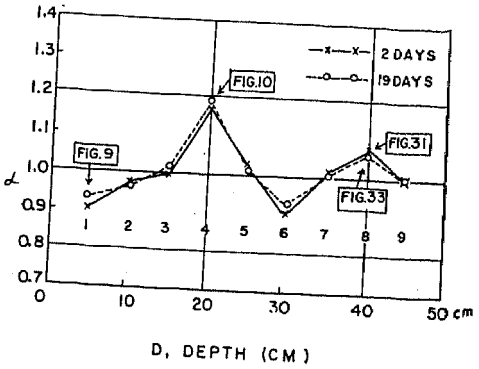

Figure 7. Deviation α of $\underline{E}$ from the E-ρ curve. Undisturbed SB, A (from Fig. 4).

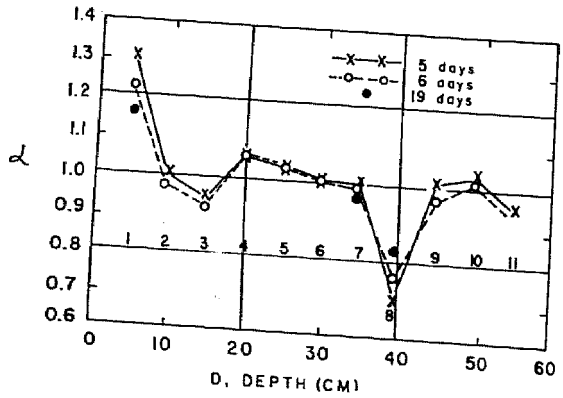

Figure 8. Deviation α of $\underline{E}$ from the E-ρ curve. Compacted SB, F (from Fig. 5).

profile and the density profile (Fig. 3). The layer of stronger bonding takes place at 20 cm and 40 cm below the surface, and the weaker bonding at 5 cm and 30 cm. No such feature is observed in the density profile. For F-series, SB compacted (Fig. 8), the curves for 5 and 6 days of hardening are almost the same and the values for 19 days agree with them, showing that the deviation from E-ρ curve is inherent in the sample.

From photomicrographs of the thin sections (Fig. 9, 10), it is clear that sample A4 (19), which shows an extraordinarily high $\underline{E}$, has more and much thicker bonds than A1 (19), which has a lower $\underline{E}$ than the average. This shows that Young's modulus is determined by three factors: density, age, and mode of bonding. The mode of bonding is determined by the number and size of bonds. This point will be treated separately.

Samples F1 and F1', SB compacted (Fig. 5) always show very high values of Young's modulus and F8 and F8' very low values. The structure of F8' (6), which has an exceptionally low value of $\underline{E}$, is granular and few minute particles are observed (Fig. 11). The number of bonds is also small. Sample F1' (6), which has an extraordinarily high $\underline{E}$, is quite different (Fig. 12), having many minute particles bonded to each other. This shows that the presence of minute particles is favorable for strengthening the processed snow, as the number of bonds becomes very large in this case.

Elastic properties and internal structure of Peter snow

An undisturbed Peter snow deposit (without chute) usually has lower densities than the Snowblast snow (with chute), ranging between 0.51 and 0.42 g/cm³. The E-ρ relation is shown in Figure 13 for the E-series. The form of the curve and the trend of age hardening are similar to the results obtained in 1958.

A block cut from the new deposit of Peter snow was brought into the undersnow laboratory at -8C ±2C and cut into three parts. The first was left on the table without any weight, the second with a load of $p = 35$ g/cm², and the third with $p = 70$ g/cm². The sample was too soft in the initial stage to be cut into a bar for Young's modulus

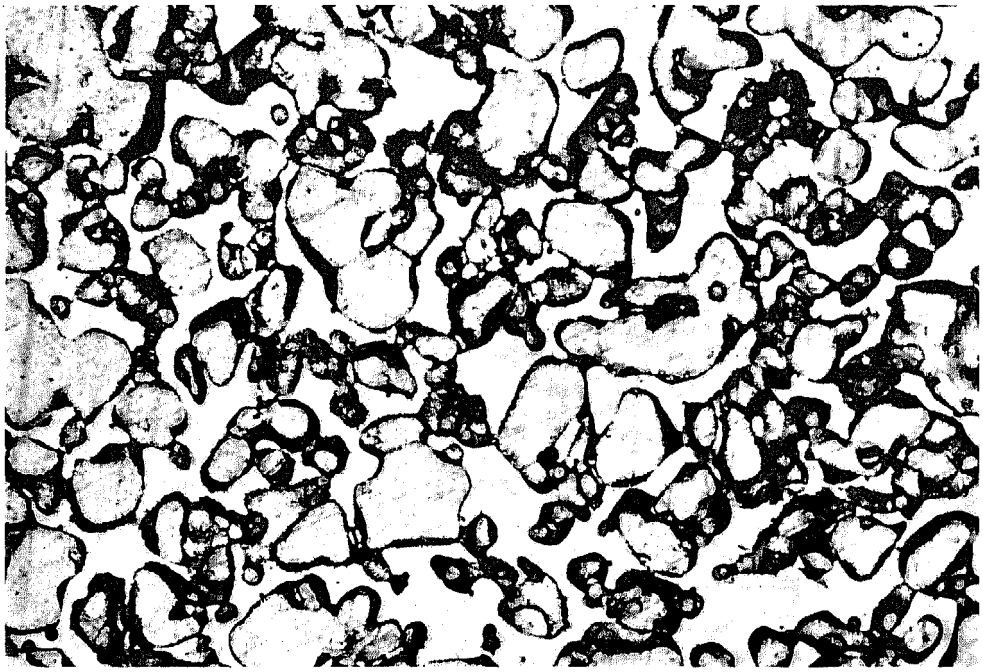

Figure 9. SB undisturbed, A1. $\rho = 0.479$, $t = 19$ days, $\alpha = 0.93$, x17.6, no. 337.

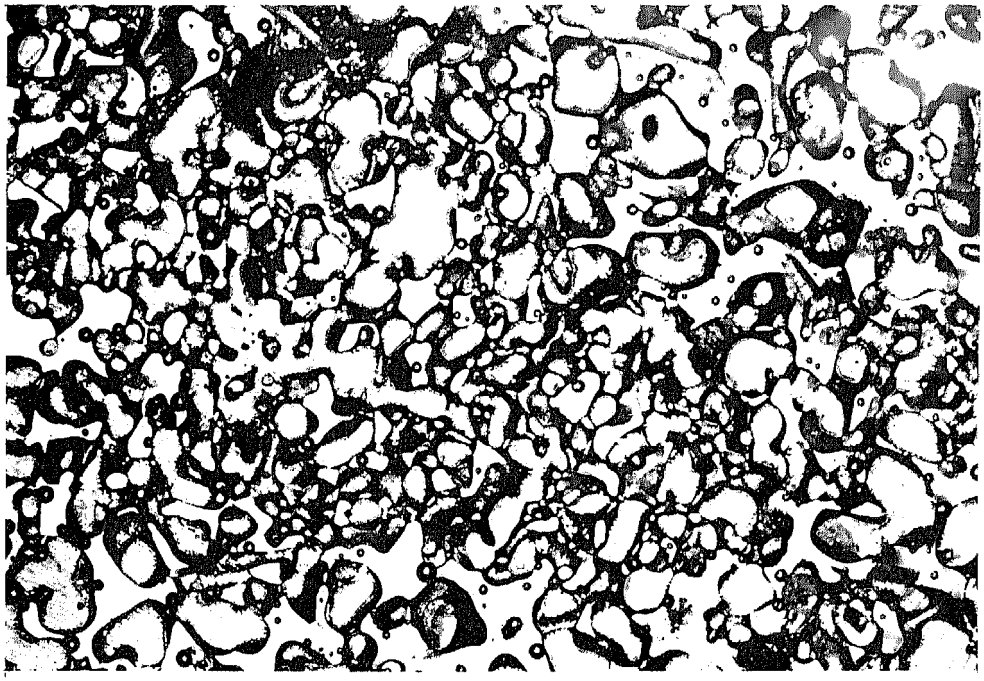

Figure 10. SB undisturbed, A4. $\rho = 0.484$, $t = 19$ days, $\alpha = 1.19$, x18.1, no. 346.

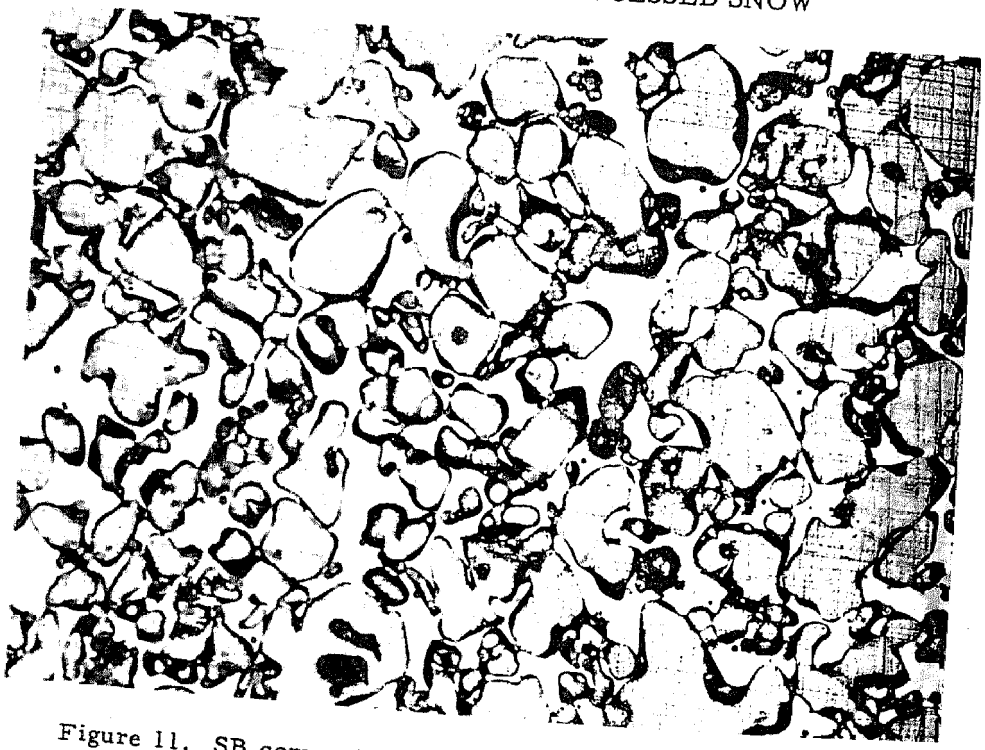

Figure 11. SB compacted, F8'. $\rho = 0.553$, $t = 6$ days, $\alpha = 0.76$, x18.1, no. 405.

Figure 12. SB compacted F1'. $\rho = 0.547$, $t = 6$ days, $\alpha = 1.30$, x18.1, no. 408.

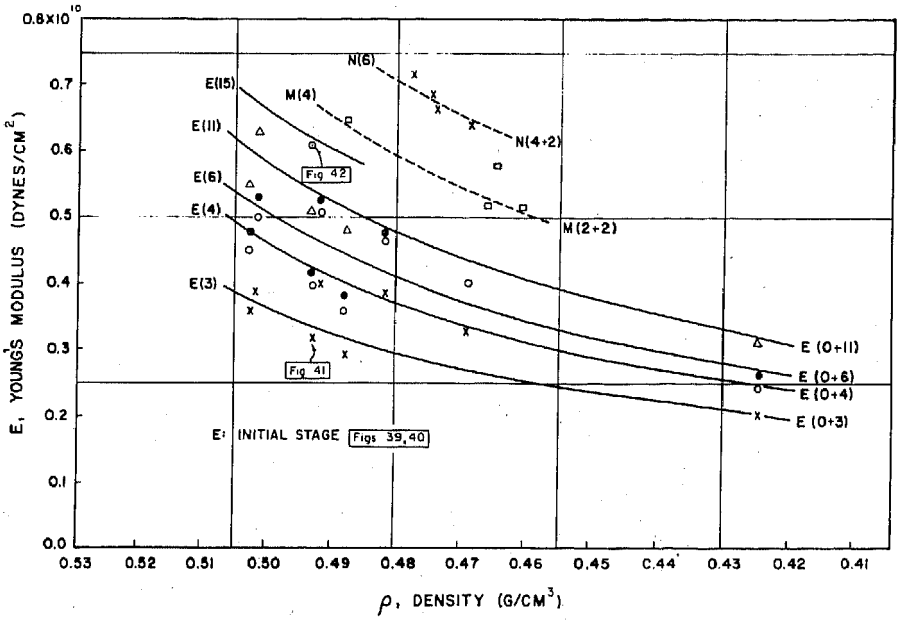

Figure 13. E-ρ relation. E, undisturbed Peter snow.

determination. The first E determination was made 8 days after deposition. It is clearly seen (Fig. 14) that the age hardening effect is accelerated by the load applied. The 10-day old sample without load (Fig. 15) has many fewer bonds between grains than similar Peter snow loaded with $p = 70$ g/cm^2 (Fig. 16). Bonding is accelerated when a load is applied. This point must be taken into account when age hardening of a thick layer of processed snow is discussed.

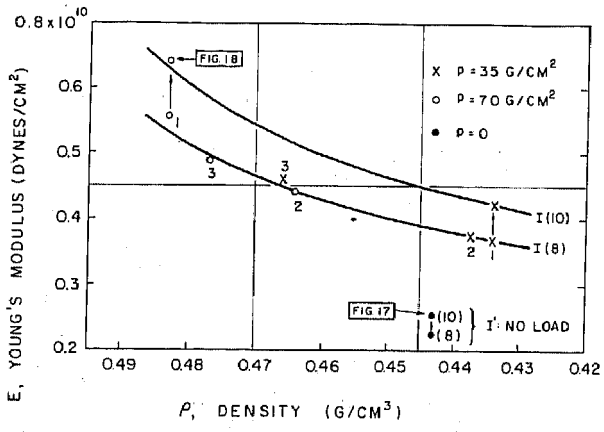

Figure 14. E-ρ relation, effect of load. I, undisturbed Peter snow.

One-year old Peter snow

Some samples whose Young's modulus was measured in 1958 were left in the undersnow laboratory for a year in plastic bags. No change in the shape was detected. Four types of samples; a-h, *l*, V, W-Z, were measured.* The result for the V-series is shown in Figure 17.

In Figure 17, the value of 1-yr-old snow is shown by a heavy line. The E-ρ relations for 7-, 10-, and 15-day-old snow are the results of the 1958 experiment. The high value of E is considered to be due to strong bondings between grains. The internal structure of sample V2 is shown in Figure 19. This sample is an example of a high Young's modulus, $E = 0.73 \times 10^{10}$ cgs. Air voids predominate because the density is low. Young's modulus, however, is high compared to the density owing to the full development of bonding. Bonding is so well developed that the snow shows a structure like a network of ice rods.

* For details of the samples, see Nakaya (1960), p. 3.

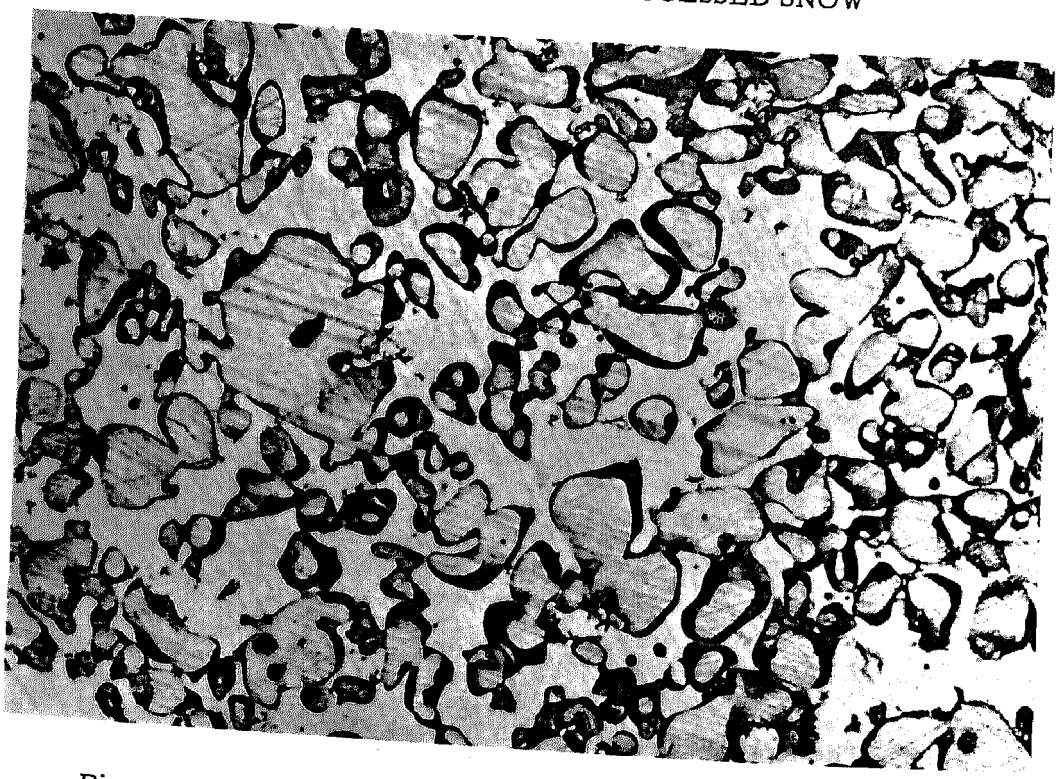

Figure 15. Peter snow I', no load. $\rho = 0.444$, $t = 10$ days, $d = 0.08$ mm, x17.6, no. 493.

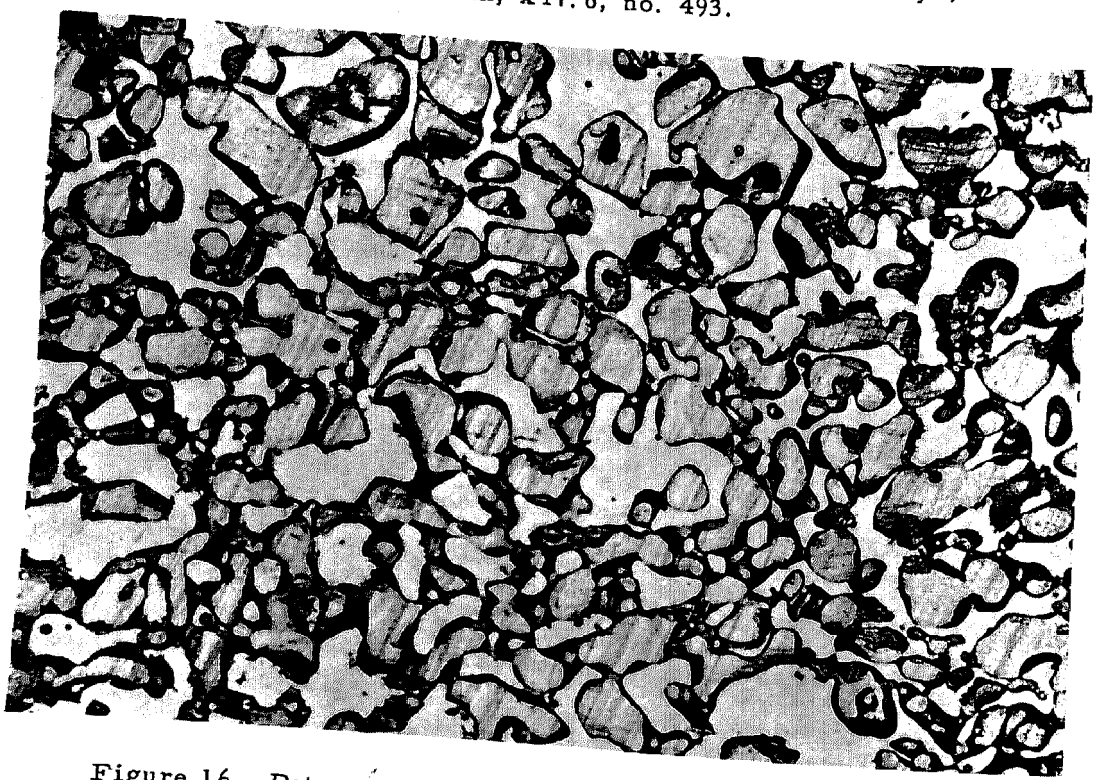

Figure 16. Peter snow I. $p = 70$ g/cm^2, $\rho = 0.483$, $t = 10$ days, $d = 0.13$ mm, x17.6, no. 497.

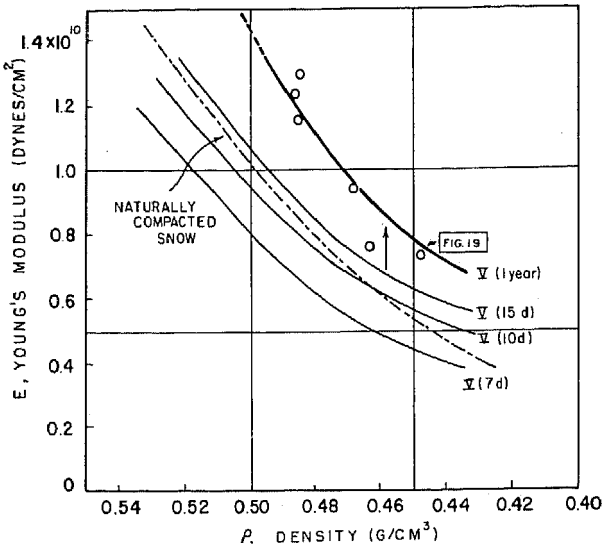

Figure 17. E-ρ relation of V-series. PS left in the laboratory for 1 yr.

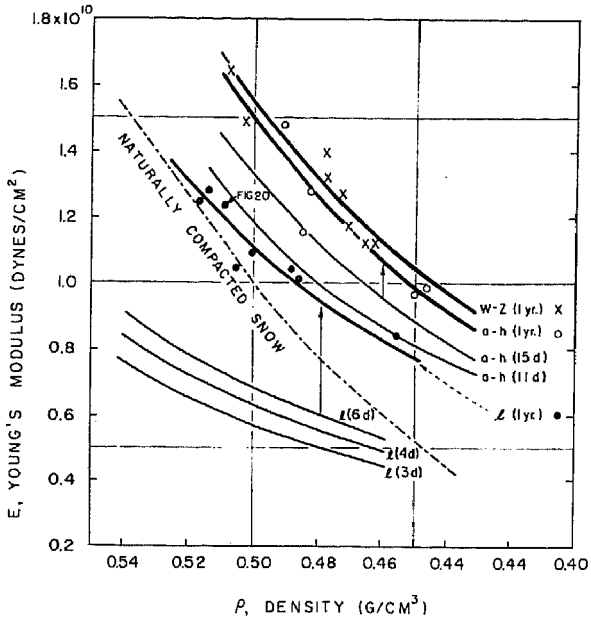

Figure 18. E-ρ relation of ℓ, a-h, W-Z series. PS left in the laboratory for 1 yr.

The E-ρ relation for ℓ, a-h, and W-Z are shown in Figure 18. The heavy lines are data for 1959, and the light lines for 1958. The series a-h and W-Z showed very high values of E in the 1958 experiment, because of the heterogeneity in size distribution of grains. The increase in E during one year is not so marked. It is about 10% for the series a-h and W-Z.

The ℓ-series showed the normal value of E in the 1958 experiment. The increase in E during one year was much larger compared with the a-h and W-Z series.

Sample ℓ5 is an example of high density and large Young's modulus; $E = 1.23 \times 10^{10}$ cgs, $\rho = 0.510$. The internal structure of this sample after one year is shown in Figure 20. The volume of air voids is markedly less than that of V2 (Fig. 19) and the bonds are very well developed. The comparatively large grains are bonded together with a network of ice rods heavier than sample V2. The internal structure is similar to that of a sample taken from about 20 m depth in naturally compacted snow, which is almost 30 years old.

Peter snow left in the field one year

Some Peter snow deposited in 1958 was left in the field untouched. These deposits were excavated in the summer of 1959, and the profiles were examined. The new snow that covered the Peter deposit was removed shortly before the examination.

Profile of undisturbed PS. The profile of an undisturbed layer (0-series) 120 cm thick was studied. Young's modulus and density of 23 samples from various strata were measured (Fig. 21). The parallel between E and ρ is very regular. Roughly speaking, this deposit is composed of two layers. From 0 to 70 cm, both E and ρ increase with depth. Maximum E is observed at D = 70 cm. In the lower layer 70 - 120 cm, both E and ρ decrease with the depth.

The internal structure varies in different strata. Snow near the top (Fig. 22), which has a low Young's modulus, shows a somewhat granular structure and the number of bonds is small, although bonding is well developed for many grains. Traces of crystalline facets are seen. They are due to sublimation of snow to a more granular condition.

The structure of snow near the middle of the deposit, which shows a high value of E, is quite different (Fig. 23). All grains are rounded in form and the bonds are not only abundant but each one is very well developed. A high Young's modulus is expected for a sample with this structure. In the lower layer, the granular nature is again

Figure 19. Peter snow, V2; t = 1 yr, ρ = 0.448, x17.6, no. 260.

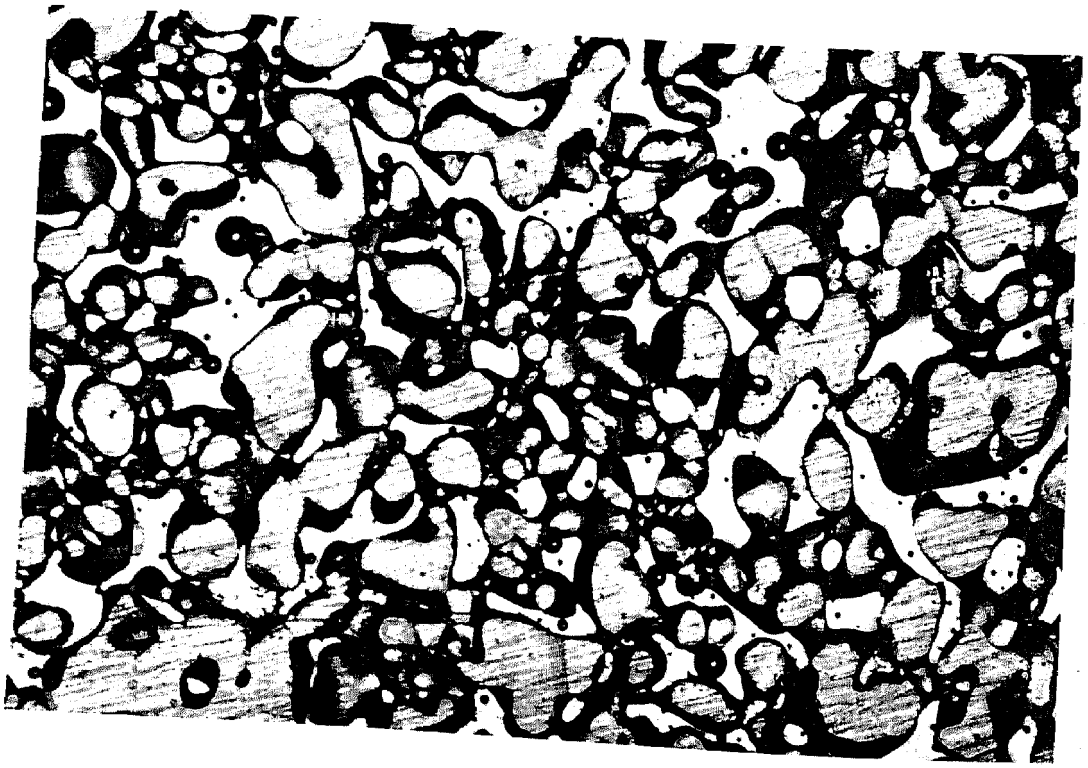

Figure 20. Peter snow #5, t = 1 yr, ρ = 0.510, x17.6, no. 267.

slightly apparent. In one example (Fig. 24) from near the bottom of the deposit, most of the bonds are fairly well developed, but some show a trace of evaporation. The number of bonds is much smaller than in the middle layer. The shape and arrangement of grains show that vapor transfer must have taken place in this layer. The general trend of the profile will be discussed later (Fig. 27).

A layer of depth hoar was observed just beneath the Peter deposit. The layer was so fragile that Young's modulus could not be measured. The structure is an assemblage of separated grains, and few bonds are observed (Fig. 25). Crystalline facets are well developed, showing that extensive sublimation has taken place. A layer of depth hoar is always observed beneath a deposit of processed snow, and the mechanism of its formation is another problem to be studied.

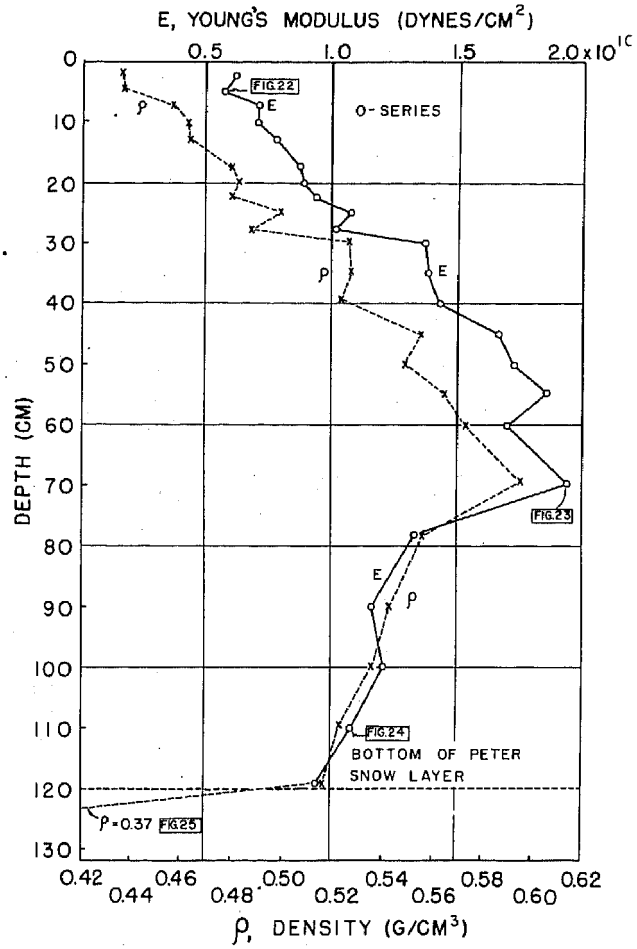

Figure 21. Profile of undisturbed PS; O-series. Left for 1 yr in the field.

Profile of PS compacted. Profiles were made at two places in compacted Peter snow. The thickness of the deposit was 80 cm. The profile (Fig. 26) is quite different from Figure 21. Both Young's modulus and density are very high near the surface and decrease with depth. At about 30 or 40 cm, $\underline{E}$ and ρ of the compacted deposit are almost the same as in the undisturbed snow. Below 30 cm depth, $\underline{E}$ and ρ are almost constant for K, with a slight increase at about 50 cm depth. In the H'-series, however, $\underline{E}$ decreases rapidly below the level of about 40 cm. This is due to a depth hoar layer at 55-60 cm depth, where $\underline{E}$ shows the minimum value.

General trend of profile. The general trend of the profile is shown in Figure 27 for the undisturbed O-series and the compacted K-series. In the undisturbed deposit $\underline{E}$ increases with depth and then decreases after passing a gradual maximum. The density curve shows a form similar to the $\underline{E}$ curve. In the whole deposit, $\underline{E}$ varies in a wide range of nearly 0.5 to 2.0 x 10^{10} dynes/cm^2. This variation is very large compared with that of the new PS deposit, and must be due to sublimation in the deposit during the year in the field. This is supported by photomicrographs of the internal structure (Fig. 22-24).

The profile of the compacted PS deposit, K-series, is also shown in Figure 27. It is interesting to note that below the level of about 40 cm both $\underline{E}$ and ρ show a trend similar to those of the undisturbed snow. Above this level, however, the profiles show contrary tendencies. The values increase toward the surface of compacted snow and decrease in the undisturbed snow. This difference must be caused by compaction.

In Fig. 27, the $\underline{E}$ vs $\underline{D}$ curve B'C' for compacted snow is extrapolated in the range B'A'' by following the trend of the range BA of the undisturbed snow. The effect of compaction is shown by the difference between the two curves A'B' and A''B'. A similar phenomenon is observed also for the density profile. The effect of compaction is shown by the difference between F'G' and F''G'.

These results indicate that mechanical compaction increases ρ and $\underline{E}$ to a depth of about 40 cm, with the effect increasing towards the surface. The difference in the absolute values of $\underline{E}$ or ρ at B'B or G'G is due to differences in the nature of the original snow or a slight change in the ambient condition while the deposit was forming.

Figure 22. Peter snow undisturbed, O; t = 1 yr in the field, D = 5.2 cm, ρ = 0.437, x14.8, no. 350.

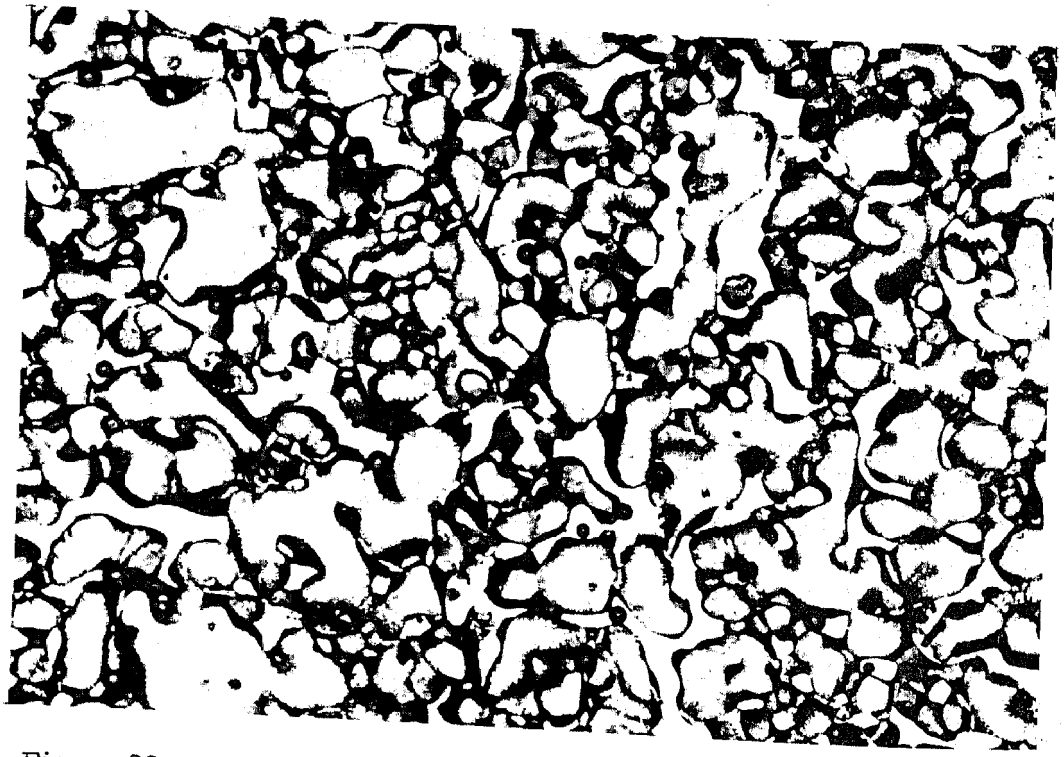

Figure 23. Peter snow undisturbed, O; t = 1 yr in the field, D = 70 cm, ρ = 0.595, x14.8, no. 354.

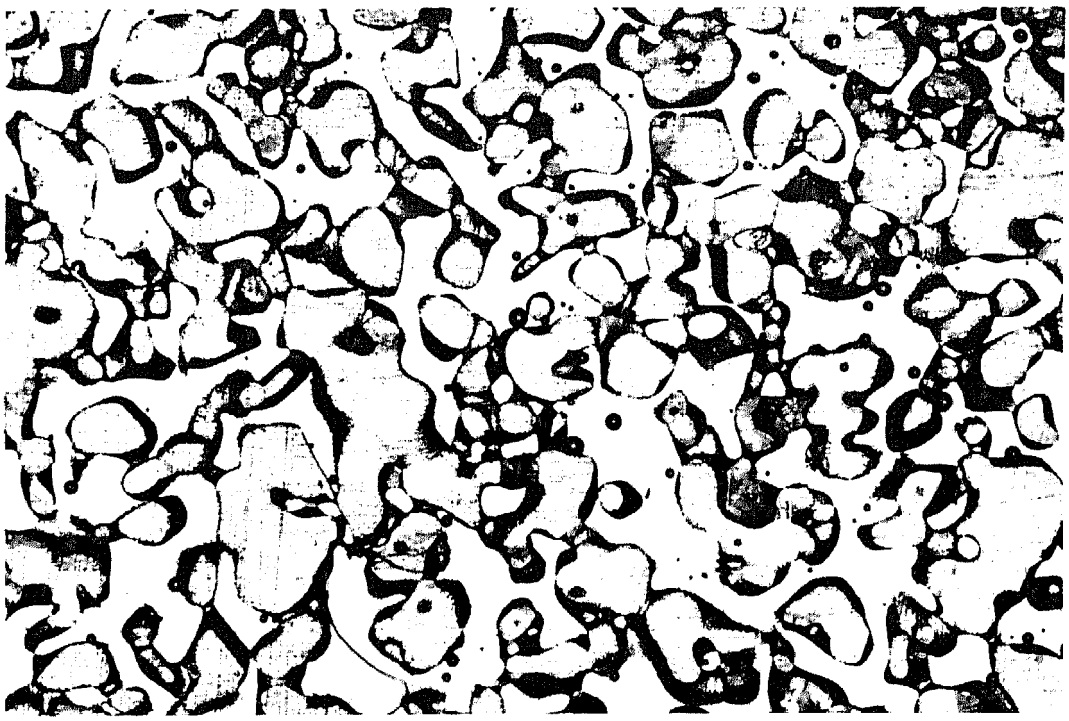

Figure 24. Peter snow undisturbed, O; t = 1 yr in the field, D = 110 cm, ρ = 0.523, x14.8, no. 356.

Figure 25. O; Granular snow beneath the PS layer. D = 125 cm, ρ = 0.37, x14.8, no. 348.

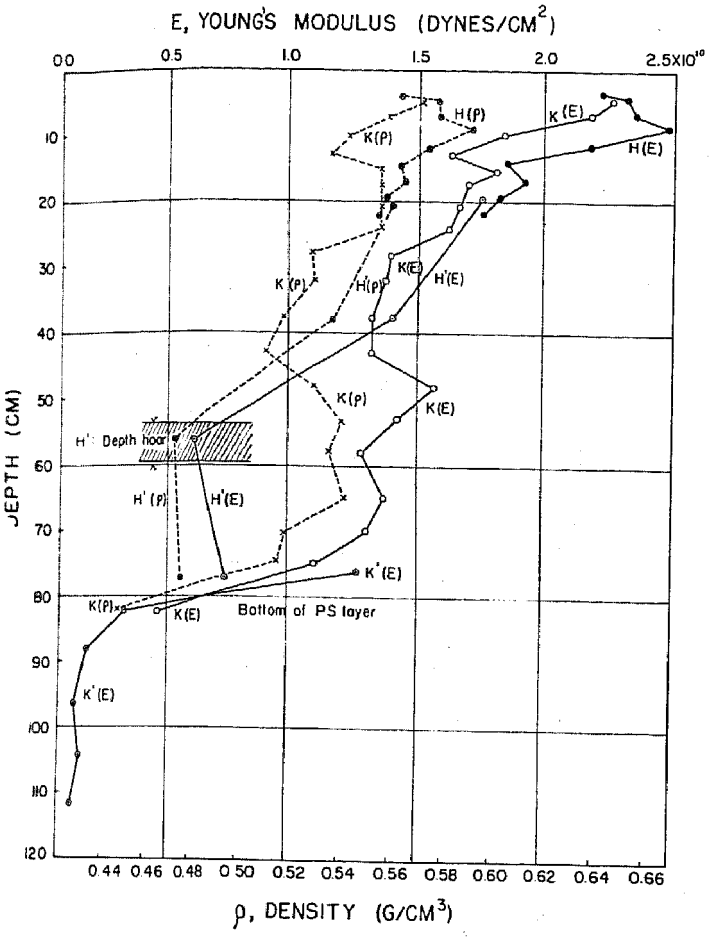

Figure 26. Profile of PS compacted; H, H', K, K'-series. Left in the field for 1 yr.

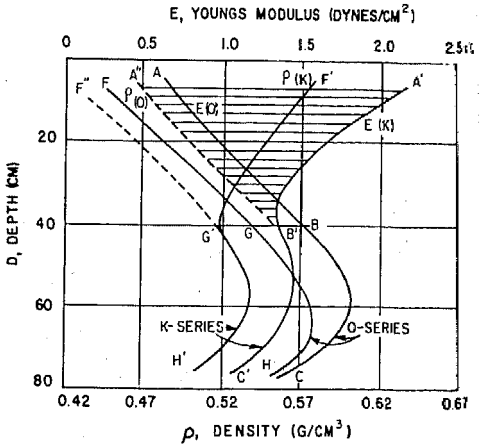

Figure 27. General trend of profile, undisturbed O-series and compacted K-series. (Smoothed curves from Fig. 21, 26.)

Relation between Young's modulus and density. The E vs ρ relation for undisturbed and compacted PS is plotted (Fig. 28). All points are scattered in the neighborhood of the E-ρ curve for naturally compacted snow. The maximum deviation is about +15% of the standard value: that is, E of naturally compacted snow of the same density. The granular samples show lower values of E. The O-series samples below 80 cm depth belong to this category (line AB, Fig. 28).

Young's modulus as a function of density and age

The E-ρ relations for various types of processed snow (Fig. 4, 5, 13, 17, 18, 28) are summarized in Figure 29. All types show the same tendency as a first approximation. The features are as follows: In the range of density above 0.5 g/cm³, the E-ρ relation is linear. Below 0.5, E decreases with decrease in density in an exponential form. For the new deposits the phenomenon of age hardening is shown by the upwards shift of the E-ρ curve.

When the processed snow is left in the field for one year, the E-ρ relation is scattered in the area of a band, with the curve for naturally compacted snow lying inside of this band. High densities were observed in the 1-yr-old snow, the maximum being 0.59. The maximum density observed in 1958 in compacted Peter snow was 0.55. The increase in density is due to the effect of the load of overlying snow.

The PS samples left in the laboratory for one year showed very high values of E. Among these, the V, W-Z, and a-h series already showed high values of E in the previous year. This high value of E was explained by the heterogeneity of grain size. After one year the Young's modulus of these samples became very large, almost twice that of naturally compacted snow. The effect is marked in the range of low density.

Age hardening and internal structure

Age hardening of Snowblast snow. The increase of Young's modulus with time t is shown in Figure 30 for Snowblast snow. Five samples of undisturbed SB (A1, A8, B4, D1, D5) are shown. For compacted SB, the values of E corresponding to ρ = 0.550

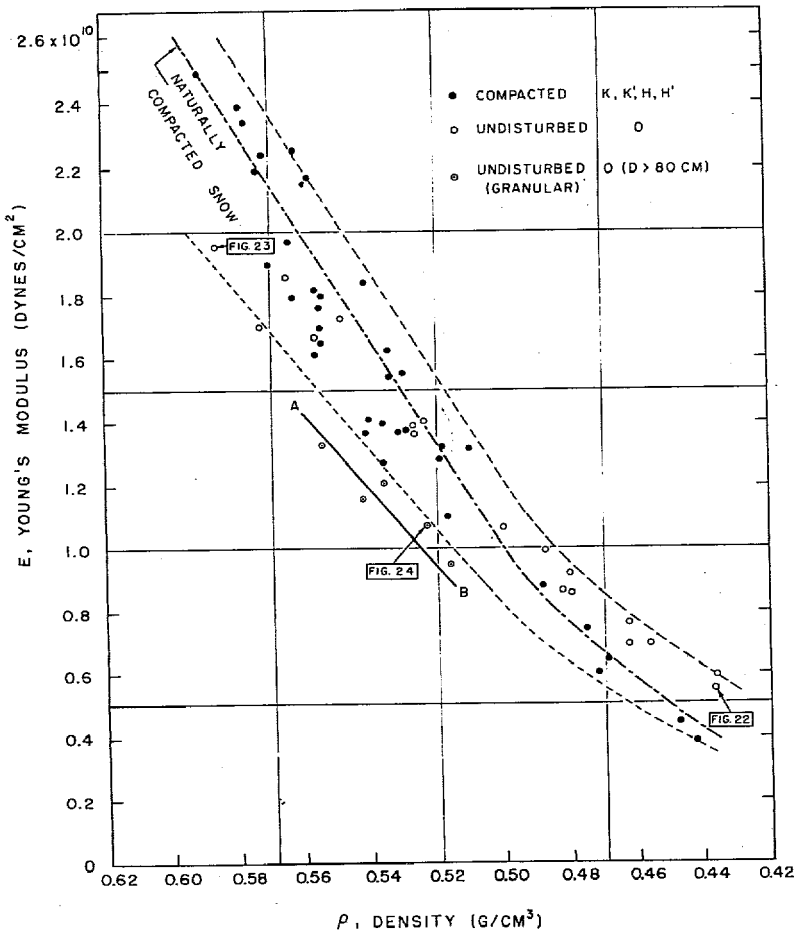

Figure 28. E-ρ relation. The undisturbed O-series and the compacted K, K'-series and H, H'-series of PS left in the field for 1 yr.

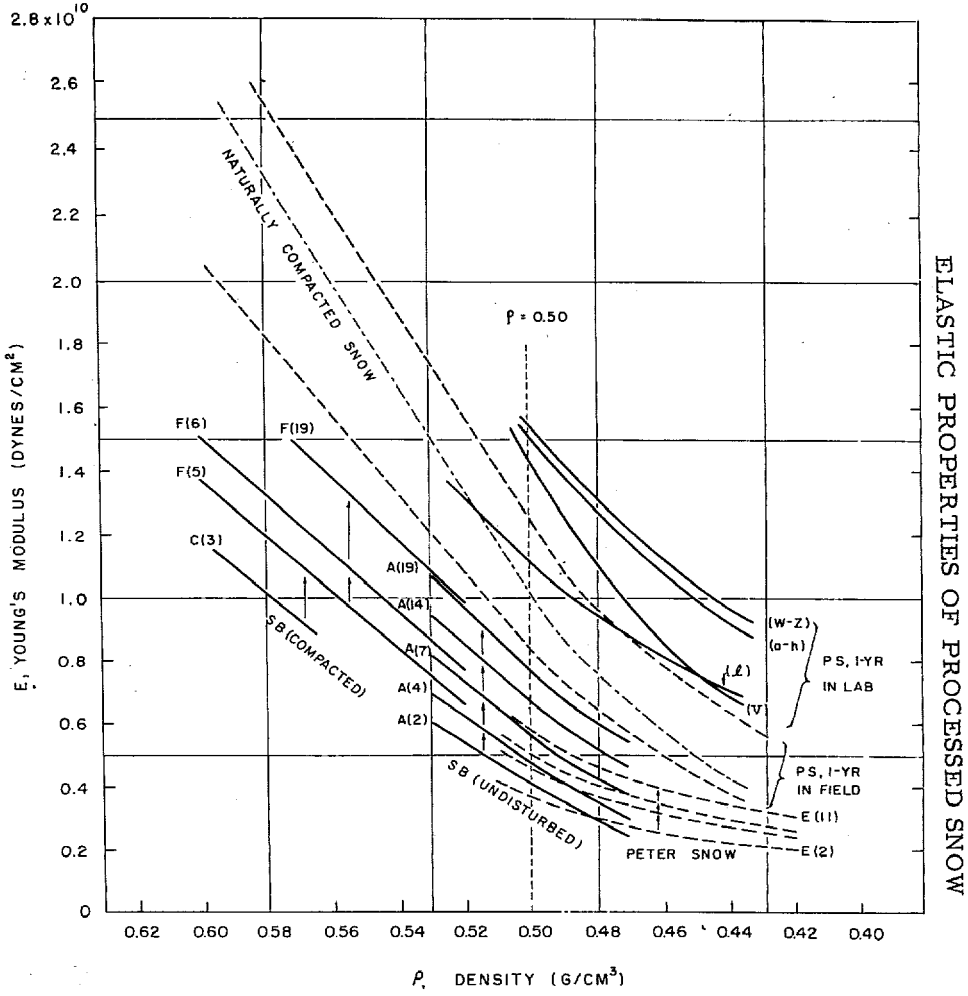

Figure 29. E-ρ relation for various kinds of processed snow.

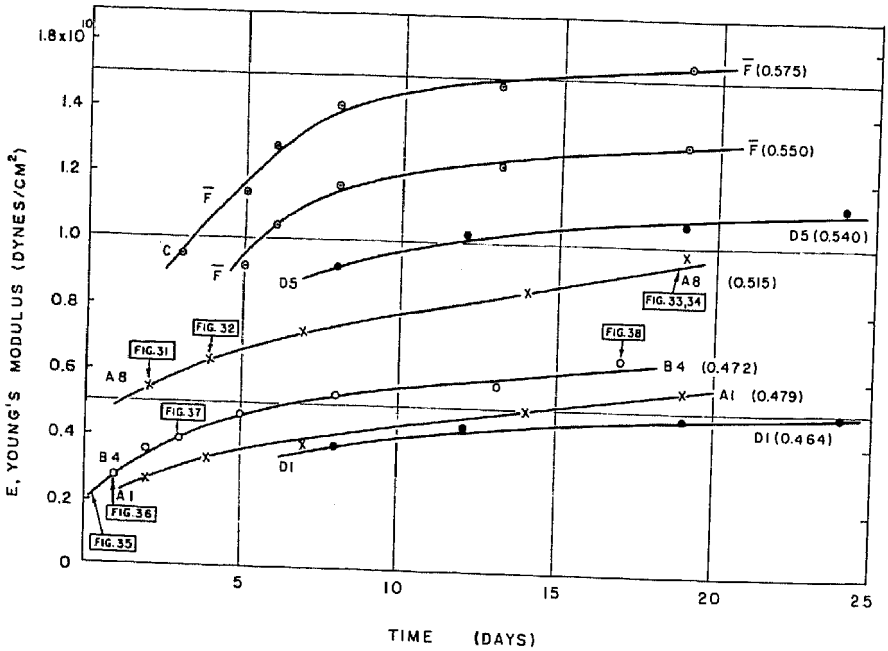

Figure 30. Age hardening of Snowblast snow, undisturbed (A, B, D) and compacted (F). Nos. in parenthesis show density, g/cm³.

and $\rho = 0.575$ are taken from the F-series curves in Figure 5. All curves show the form of a saturation curve. The trend agrees with the results obtained in 1958 for Peter snow (Nakaya, 1960, Fig. 11).

The relation between age hardening and internal structure was studied with respect to two samples of undisturbed snow A8 and B4.

Photomicrographs of A8 taken at three stages are shown in Figures 31-34. Two days after deposit (Fig. 31), large and minute grains are seen mixed with each other. Bonds between grains are observed at most of the points of contact. The average size of the bond is of the order of 0.1 mm diam. At $t = 4$ days (Fig. 32) minute particles are smaller in number than at $t = 2$ days and the bonds are more developed. The average bond size is a little over 0.1 mm.

The change in internal structure is clearly seen at $t = 19$ days (Fig. 33). Minute particles are almost gone, and the bonds are very well developed. The disappearance of minute particles is considered to be partly due to sublimation and partly to amalgamation with larger grains (discussed below). The average size of bond grew to about 0.2 mm in diameter. Usually one grain is not a single crystal, but is made of several crystals (Fig. 34). Most of the boundaries are observed in the form of a straight line. One good example is shown near the center of Figure 34. This kind of boundary is conveniently explained as the result of surface migration of H_2O molecules, as described below.

Initial stage of bonding. The initial stage of bonding was studied by solidifying the snow sample with aniline shortly after the deposit was made. One example of undisturbed SB (sample B4) is shown at $t = 2$ hr (Fig. 35), and $t = 18$ hr (Fig. 36). At $t = 2$ hr, many minute particles are observed and their shape suggests that they are produced by crushing of the snow by the snow miller. Bonding between grains is not yet noticeable, but close examination of the photograph reveals that a few bonds have already started in this stage. It is an interesting fact that bonding has already begun 2 hr after deposition. After 18 hr (Fig. 36), bonding is clearly observed. Most of the points of contact between grains are connected by ice bridges of about 0.05 mm diam. The minute particles decrease in number and become rounded. This must be caused, at least partly, by evaporation due to curvature.

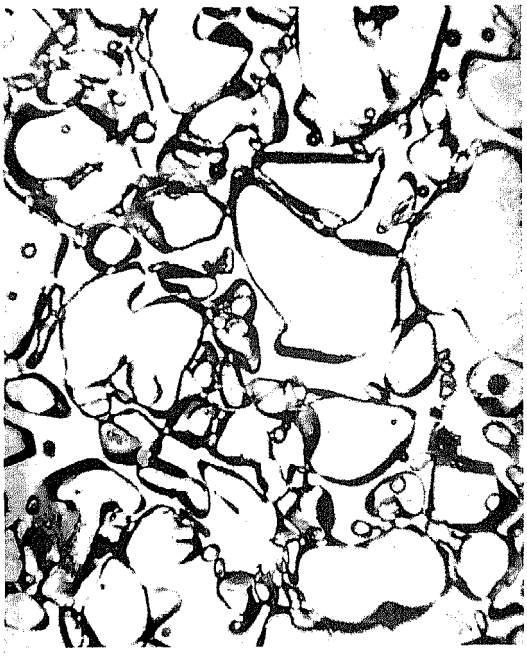

Figure 31. A8: SB undisturbed, $\rho = 0.515$, t = 2 days, x27.7, d = 0.07 mm.

Figure 32. A8: SB undisturbed, $\rho = 0.515$, t = 4 days, x27.7, d = 0.06 mm.

Figure 33. A8: SB undisturbed, $\rho = 0.515$, t = 19 days, x27.7, d = 0.08 mm.

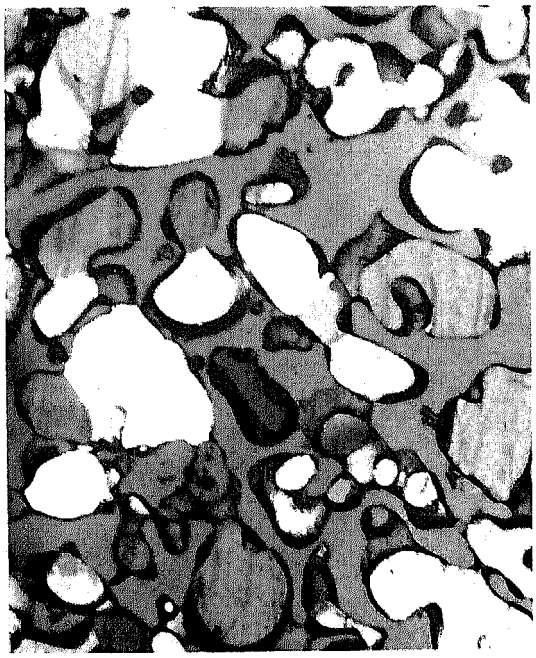

Figure 34. Same as Fig. 33, under crossed polaroids.

Figure 35. B4: SB undisturbed, ρ = 0.503, t = 2 hr, x27.7, d = 0.08 mm.

Figure 36. B4: SB undisturbed, ρ = 0.503, t = 18 hr, x27.7, d = 0.05 mm.

Figure 37. B4: SB undisturbed, ρ = 0.472, t = 3 days, x27.7, d = 0.05 mm.

Figure 38. B4: SB undisturbed, ρ = 0.472, t = 17 days, x27.7, d = 0.07 mm.

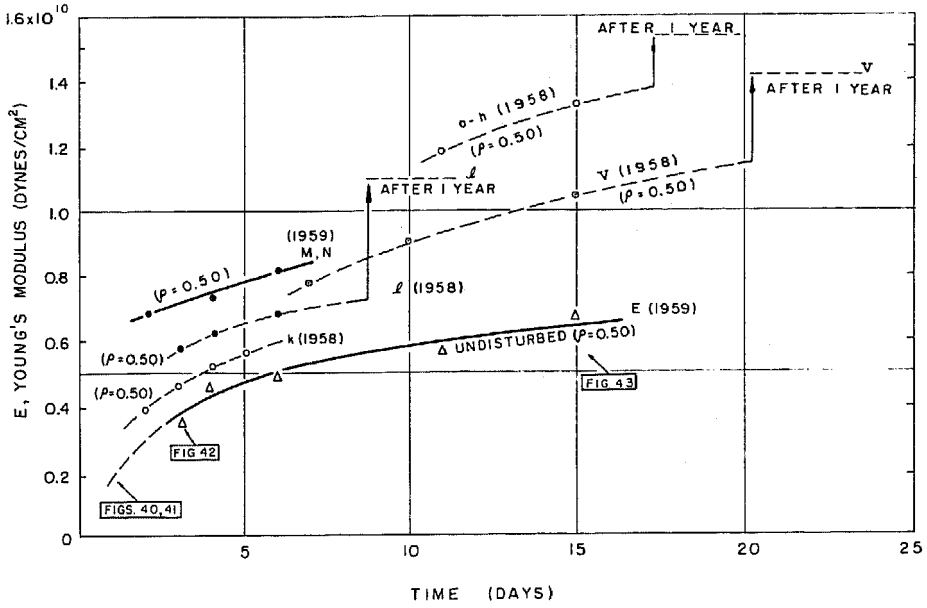

Figure 39. Age hardening of Peter snow, 1958 and '59.

Similar behavior of minute particles and mode of bonding is observed in the case of Peter snow (Fig. 40, 41). Further development of bonding is similar for SB (Fig. 37, 38) and PS (Fig. 42, 43).

Age hardening of Peter snow. The E-t curve for Peter snow is shown in Figure 39 for two series, E and M, N. Young's modulus corresponding to $\rho = 0.50$ is read from the E-ρ curve and plotted with a solid line. The trend of the curve is the same as for Snowblast snow. The internal structure at $t = 3$ days and $t = 15$ days is shown in Figures 42 and 43. Three days after deposition most minute particles have vanished and ice bridges are developed, the average diameter being about 0.1 mm. At $t = 15$ days (Fig. 43) the minute particles are all gone and the bonds are well developed. No essential difference was observed in the structure of Peter snow and Snowblast snow.

The results of experiments carried out in 1958 and of tests on samples left in the laboratory for one year are shown in Figure 39 by broken lines.

Mechanism of bonding

The mechanism of formation of ice bridges between grains is an interesting and important problem not only from the scientific point of view but also from the standpoint of snow engineering in the Arctic.

One of the features of this bridge is that in most cases the boundary between amalgamated grains takes the form of a plane, a straight line in the two-dimensional cut. One good example is given in Figure 34. Another example is shown in Figure 44.

The mechanism of formation of this kind of boundary is conveniently explained by assuming the existence of a liquidlike film on the surface of ice at temperatures below freezing. Weyl proposed this idea (1951); an experiment showing the existence of a liquidlike film on the ice surface was reported a few years later (Nakaya and Matsumoto, 1954) and confirmed by Hosler and others (Hosler, Jensen, and Goldshlak, 1957).

If we assume this liquidlike film, the development of bonding will proceed as schematically shown in Figure 47. In this case the formation of a straight boundary is expected. The boundary as shown in Figure 47c is indicated by an arrow in the photograph of Figure 45. Kingery (1959) studied the rate of growth of bonding at the point of contact of two ice spheres, and found that the welding together of ice particles occurs as a result of surface diffusion. In a similar experiment, Kuroiwa (personal

Figure 40. E5: Peter snow, $\rho = 0.493$, t = 2 hr, x27.7, d = 0.06 mm.

Figure 41. E5: Peter snow, $\rho = 0.493$, t = 21 hr, x27.7, d = 0.09 mm.

Figure 42. E5: Peter snow, $\rho = 0.493$, t = 3 days, x27.7, d = 0.07 mm.

Figure 43. E5: Peter snow, $\rho = 0.493$, t = 15 days, x27.7, d = 0.07 mm.

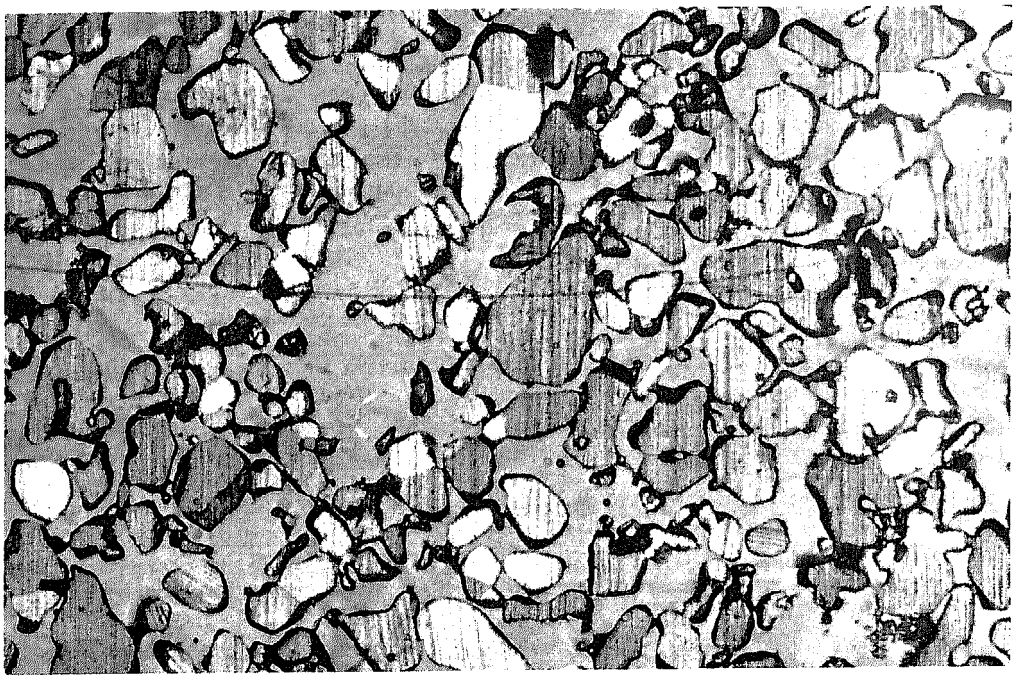

Figure 44. B4: SB undisturbed, t = 3 days, ρ = 0.472, d = 0.04 mm, x17.6, no. 573.

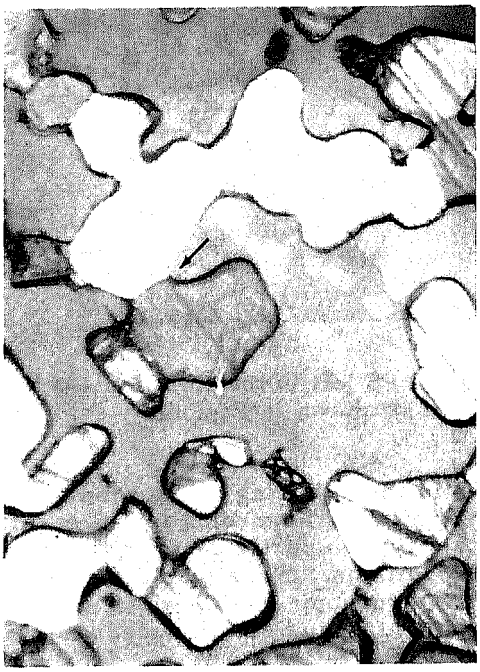

Figure 45. D1: SB undisturbed, t = 24 days, ρ = 0.464, d = 0.02 mm, x36, no. 558.

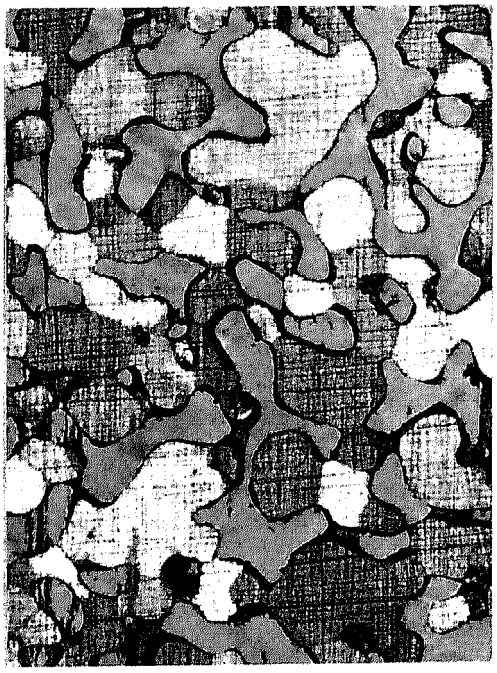

Figure 46. H1: PS in the field, t = 1 yr, ρ = 0.562, d = 0.04 mm, x17.6, no. 549, crossed polaroids.

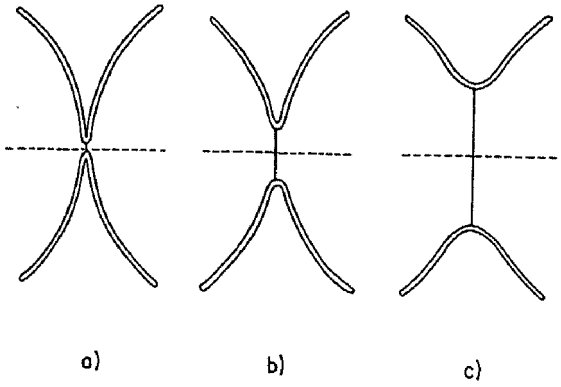

Figure 47. Model of growth of bonding by surface diffusion.

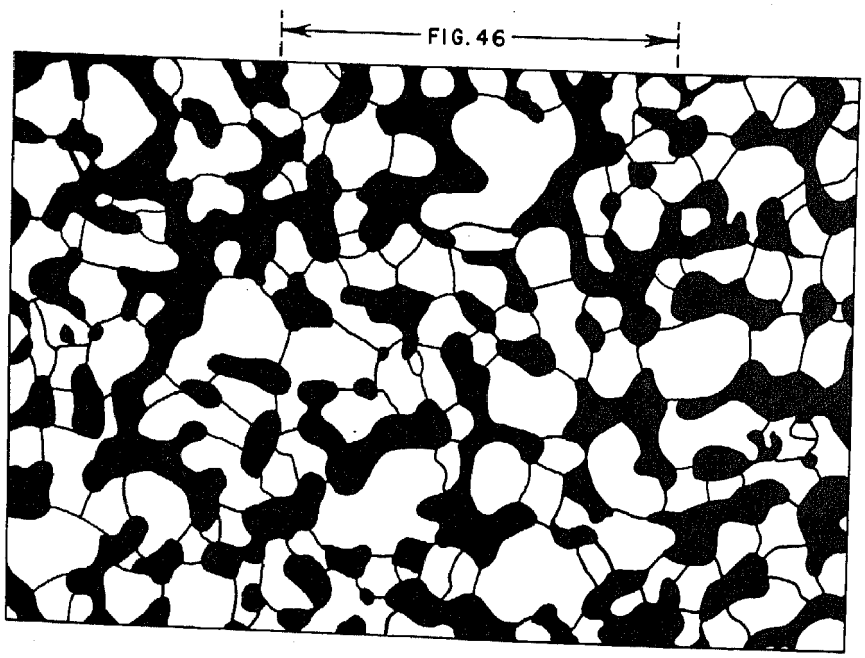

Figure 48. Sketch of arrangement of grains. PS left in the field for 1 yr; H-series. Photo of part of sample is shown in Fig. 46.

communication) studied the growth of bonding statistically during age hardening of powder snow, using the thin section method with aniline. According to his results, not yet published, sublimation as well as surface diffusion participates in the process. Sintering theory is applicable under isothermal conditions. When a small thermal gradient exists, sublimation will take place on a microscopic scale, which is effective in the growth of bonding. Further detailed experimental studies are necessary to clarify the mechanism of bonding.

When bonds develop fully, the arrangement of ice grains shows a structure like a network of ice rods. The samples left in the field for one year belong to this category (e.g. Fig. 46, 48). This is an intermediate stage of transition of snow into glacier ice. After this stage is reached, recrystallization under large pressures plays an important role in further densification.

REFERENCES

Hosler, C. L.; Jensen, D. C.; and Goldshlak, L. (1957) On the aggregation of ice crystals to form snow, Journal of Meteorology, vol. 14, p. 415-420.

Jellinek, H. H. G. (1957) Thin section analysis, U. S. Army Snow Ice and Permafrost Research Establishment, Corps of Engineers, Research Report 35.

Kingery, W. D. (1959) Regelation, surface diffusion and ice sintering, Journal of Applied Physics, 1960 (May or June).

Kinoshita, S., and Wakahama, G. (1959) (Observation of thin section of snow made by the aniline method) Seppyō, vol. 21, p. 11-14. (Text in Japanese).

Nakaya, U. (1959) Visco-elastic properties of snow and ice in the Greenland Ice Cap, U. S. Army Snow Ice and Permafrost Research Establishment, Corps of Engineers, Research Report 46.

_____ (1960) Visco-elastic properties of processed snow, U. S. Army Snow Ice and Permafrost Research Establishment, Corps of Engineers, Research Report 58.

_____ and Matsumoto, A. (1954) Simple experiment showing the existence of "Liquid Water" film on the ice surface, Journal of Colloid Science, vol. 9, p. 41-49.

Weyl, W. A. (1951) Surface structure of water and some of its physical and chemical manifestations, Journal of Colloid Science, vol. 6, p. 389-405.